*Original article*

# Morphometric assessment of the choroid in dogs diagnosed with retinal atrophy (RA) with symptoms of progressive retinal atrophy, using spectral-domain optical coherence tomography (SD-OCT)

## J. Zwolska[1], I. Balicki[1], A. Balicka[2], B. Kuduk[1]

[1] Department and Clinic of Animal Surgery, Faculty of Veterinary Medicine,
University of Life Sciences in Lublin, Głęboka 30, 20-612 Lublin, Poland
[2] Small Animals Clinic,
University of Veterinary Medicine and Pharmacy in Košice, Komenského 73, 040 01 Košice, Slovakia

Correspondence to: I. Balicki, e-mail: balicki.ireneusz@gmail.com, tel +48 603 066 376

## Abstract

The aim of the study was to determine the thickness of choroidal layers in mixed breed dogs suffering from retinal atrophy (RA) and showing symptoms of progressive retinal atrophy (PRA), with the use of SD-OCT. The study was performed on 50 dogs divided into two groups: 25 dogs diagnosed with retinal atrophy (RA) with PRA symptoms aged 1.5-14 years and 25 healthy dogs aged 2-12 years. The dogs were examined using slit-lamp biomicroscopy, tonometry, ophthalmoscopy, fundus camera and SD-OCT (Topcon 3D OCT 2000). Measurements of the choroidal layers: RPE-Bruch membrane-choriocapillaris complex (RPE-BmCc) with tapetum lucidum in tapetal fundus, medium-sized vessel layer, (MSVL), large vessel layer with lamina suprachoroidea and (LVLS) whole choroidal thickness (WCT) were taken manually with the use of the caliper function integrated with the SD-OCT software. The measurements were performed dorsally (D) and ventrally (V) at a distance of 5000-6000 μm, and temporally (T) and nasally (N) at a distance of 4000-7000 μm from the optic disc with enhanced depth scans. The measurements were conducted temporally and nasally both in the tapetal (TempT, Nast) and nontapetal (TempNT, NasNT) fundus. Statistical analysis was performed using Statistica 10 software (Mann Whitney U Test). In all dogs affected by retinal atrophy (RA) with PRA symptoms, a statistically significant (p≤0,05) reduction in thickness of MSVL was observed in all the measured regions. A statistically significant reduction in thickness of LVLS and WCT was found in all nontapetal areas (p≤0,05). RA in mixed breed dogs with PRA symptoms was accompanied by choroid disorders such as reduction in thickness of the large vessel layer and decreased whole choroidal thickness in the nontapetal fundus as well as the medium vessel layer in all fundus regions.

**Keywords:** canine, choroid, choroidal thickness, optical coherence tomography, retinal atrophy

## Introduction

Canine retinal degenerative diseases are differentiated between the hereditary, progressive retinal atrophy (PRA) and the non-hereditary, postinflammatory retinal degenerations. Ophthalmoscopic features of PRA are bilateral symmetry and progressivity. Asymmetrical, sometimes non-progressive, local or widespread nature is characteristic for the other lesions that can be associated with inflammation, infection or toxicity (Barnett et al. 1983, Maggs et al. 2017). In the post-inflammatory retinal degeneration the areas of retinopathy may be limited to one eye, or both eyes might be affected but not to the same degree. Known causes of post-inflammatory retinal degeneration include infectious diseases, such as canine distemper, toxoplasmosis, cryptococcosis, blastomycosis, leishmaniasis and histoplasmosis. Retinal degeneration may also occur in systemic diseases such as diabetes mellitus and nephritis. It may be also associated with such conditions as lens luxation or intraocular tumours (Barnett et al. 1983, Maggs et al. 2017). The telltale symptoms of PRA observed during ophthalmoscopic examinations of the fundus include hyperreflectivity – observed in the early stages of the disease – followed by initially localized, and later general, reduction in thickness and atrophy of blood vessels, abnormal retinal pigmentation, and atrophy of the optic disc. The changes occur symmetrically and bilaterally (André et al. 2008, Downs et al. 2014). It is commonly accepted that PRA begins peripherally and progresses toward the center of the fundus. As follows from our previous research, retinal atrophy in dogs suffering from PRA starts in the ventral region, in the nontapetal region, and spreads above the optic nerve into the region of the tapetum lucidum (Balicki et al. 2018).

Due to its phenotypic similarity, retinitis pigmentosa (RP) diagnosed in people is considered the human counterpart of canine progressive retinal atrophy. The group of diseases generally classified under the category of retinitis pigmentosa are characterized by the hereditary and progressive character of the lesions, presence of "bone spicule pigmentation", reduced field of vision, deterioration of low light vision quality, and reduced photoreceptor response during an electroretinography exam (Poornachandra et al. 2019). Twilight blindness is related to the loss of rod cells in the early stage of the disease which, ultimately leads to atrophy of the entire photoreceptor layer, starting from the peripheral areas of the retina and ending with the macular receptors (Liu et al. 2016, Milam et al.1998). Upon closer analysis, scans taken with the use of spectral-domain optical coherence tomography (SD-OCT) reveal decreasing thickness of the external photoreceptor layer. As follows from the studies conducted to date, RP can also be associated with degeneration of the choroid (Adhi et al. 2013, Finzi et al. 2014, Poornachandra et al. 2019, Korte et al. 1984). Previous results in patients diagnosed with RP showed a preferential reduction in thickness of the large choroidal vessel layer. RP was characterized by variable choriocapillaris atrophy. The shape of the choroid was irregular (Shintani et al. 2009, Oh et al. 2020)

Recent advances in choroid imaging techniques, including enhanced depth imaging optical coherence tomography, have facilitated a more thorough analysis of this structure (Singh et al. 2019). Histologically, the choroid can be divided into between four and six layers, depending on whether the vascular region is treated as a single or double layer, and whether it is assumed that the lamina fusca is a part of the sclera or the choroid. In most household mammals, dogs included, starting from the retina (the inner section) the choroid is composed of Bruch's membrane, the choriocapillaris, tapetum lucidum, intermediate--vessel layer, large-vessel layer and the suprachoroidea (Nickla and Wallman 2010, McLellan and Rasmussen 2012, Rosolen et al. 2012).

SD-OCT is a contactless and non-invasive method that facilitates fast, cross-sectional, real-time, in vivo imaging of the retina and the choroid (Gabriele et al. 2011, Xu et al. 2017). SD-OCT choroidal imaging in dogs, however, is a new area of study. As a multi--purpose structural element of the eyeball, the choroid can be affected by pathological processes that may have a direct bearing on the visual function (Bruè et al. 2013, Murthy et al. 2016, Brusini 2018). In a previous study conducted on clinically healthy dogs, it was demonstrated that the SD-OCT method is the perfect tool for non-invasive, in vivo imaging of the choroid as well as morphological and morphometric assessment of its condition. Moreover, SD-OCT allows one to discern the respective layers of the canine choroid. It has also been demonstrated that the total thickness of the choroid, as well as its respective layers does not change with the age (Zwolska et al. 2021, 2023).

The aim of the present study was to analyze the thickness of respective choroidal layers in particular regions of the eye in dogs suffering from retinal atrophy (RA) with PRA symptoms and compare the results to those obtained from healthy dogs. As it was impossible to establish PRA heredity in particular mixed breed dogs included in the study, the authors chose to describe the diagnosed condition as retinal atrophy (RA) with PRA symptoms.

## Materials and Methods

### Animals

The study was performed on 50 mixed breed dogs divided into two groups: 25 dogs diagnosed with retinal atrophy (RA) with PRA symptoms aged 2-12 years, 18 males and 7 females (RA) and 25 healthy dogs aged 2-12 years, 15 males and 10 females, as the control group (Control). The animals were patients of the Department and Clinic of Animal Surgery at the University of Life Sciences in Lublin. The owners were informed of the nature of the examinations and gave their consent. The research was approved by the Scientific Research Committee of the Department and Clinic of Animal Surgery at the University of Life Sciences in Lublin on February 1, 2018 (#6/2018) in a decision concerning non-experimental clinical patients. The study was performed in accordance with Polish law and Directive 2010/63/EU of the European Parliament and of the Council of 22 September 2010 on the protection of animals used for scientific purposes, Chapter I, Article 1, point 5(b).

### Clinical examination

All the dogs were classified as healthy based on physical examinations and blood test results. The blood tests included complete blood cell counts, urea, complete bilirubin, creatinine, aspartate transaminase, alanine transaminase, alkaline phosphatase, and amylase. Only animals whose results were within the reference ranges were qualified for the study. The dogs had been dewormed twice a year. The examinations did not indicate that the dogs had previously suffered from any systemic or ophthalmic disorders.

### Ophthalmological examination

Ocular examination was performed using a slit lamp biomicroscope (Shin-Nippon, Japan). Intraocular pressure (IOP) measurements were obtained using a rebound tonometer TonoVet (iCare, Finland). Only animals with an intraocular pressure (IOP) within the range of 15-20 mmHg were qualified. The pupillary light reflex, both direct and consensual, chromatic pupillary light reflex, menace response and dazzle reflex were estimated in all the dogs. Behavioral ophthalmic tests included tracking and placing or obstacle tests under scotopic and photopic conditions. Fundus examination was performed using a binocular indirect ophthalmoscope (Keeler, UK), direct ophthalmoscope (Welch Allyn, USA), and a panoptic ophthalmoscope (Welch Allyn, USA). Photographs of the ocular fundus were taken using a Handy NM-200D Fundus Camera (Nidek, Japan) connected to a computer operating IrfanView software (Wiener Neustadt, Austria). No vision impairment or ocular abnormalities were identified in any dogs from the Control group.

### Preparation of animals for electroretinography

All dogs from the RA group underwent an electroretinography (ERG) exam (RETIportERG: Acrivet; Hennigsdorf, Germany). The animals fasted for at least 12 hours prior to the ERG recording. Bright sunlight was avoided for a minimum of 2 hours prior to the procedure. Maximal pupillary dilation was obtained by applying eyedrops containing 1% tropicamide (Tropicamidum 1%, WZF Polfa S.A., Poland). The dogs were sedated with an intramuscular injection of medetomidine at a dose of 0.03 mg/kg (Cepetor 1 mg/mL, CP Pharma, Germany). General anesthesia was induced with an intramuscular injection of ketamine (Vetaketam 100 mg/ml, Vet-Agro Sp. z o.o., Poland) at a dose of 5 mg/kg. When prolonged general anesthesia was required, ketamine was administered intravenously as needed. After intubation, the dogs were placed in sternal recumbency. Heart and respiratory rates, electrocardiographic trace and pulse oximetry were measured using a multiparameter monitor.

### ERG procedures

The canine protocol endorsed by the European College of Veterinary Ophthalmologists was used (Ekesten et al. 2013). Steel subdermal needle electrodes (BIONEN S.a.s., Italy) were used to record the ERG. A reference electrode was placed approximately 2 cm caudally to the lateral canthus of the tested eye and a ground electrode was placed over the external occipital protuberance. The cornea was anesthetized with a local administration of 0.5% proparacaine hydrochloride (Alcaine®, Alcon Inc.). A drop of 2.5% hypromellose solution (GONIOVISC, HUB Pharmaceuticals, LLC, Rancho Cucamonga, CA) was placed on the cornea to keep it moist and facilitate electrical conduction with the ERG electrode. A contact lens with built-in electroluminescent diodes served as the active electrode (LED, Kooijman/Damhof ERG lens®, Medical Workshop BV, Groningen, The Netherlands). All the lights in the room were switched off before the ERG exam started.

Each ERG session included scotopic and photopic ERG. The rod response was evaluated under scotopic adaptation during a 20-minute adaptation period. Response to the stimulation using a light impulse with an intensity of 0.03 cd*s*m$^{-2}$ was measured 5 times, every 4 minutes. A 10 Hz rod flicker was observed at the same level of stimulation. The mixed rod and cup
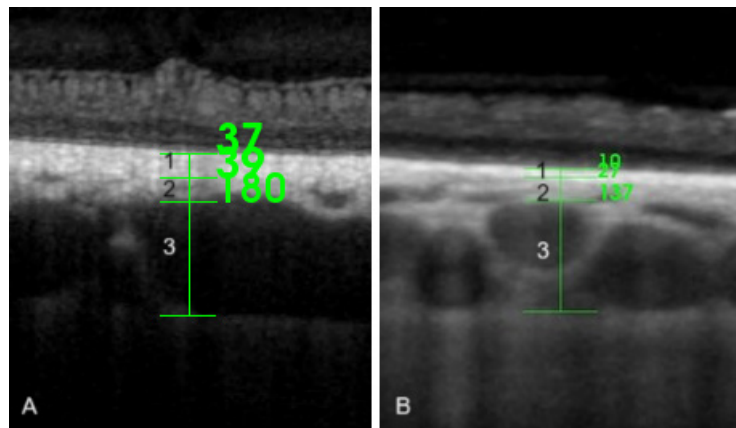
Fig. 1. Measurement of the respective choroidal layers (1 – RPE-BmCc, 2 – MSVL, 3 – LVLS) in dogs suffering from retinal atrophy (RA) in the tapetal (A) and nontapetal region (B).

response was recorded under scotopic adaptation using light flash stimulation with an intensity of 3 cd*s*m$^{-2}$. Photopic response was recorded with background illumination at a level of 30 cd*m$^{-2}$, using a standard 3 cd*s*m$^{-2}$ impulse. To obtain the transient response result, 3 individual flashes were averaged, while the flicker response was measured using 31 Hz light-flash stimulation.

The reference values for the ERG wave amplitude and latency were obtained from the control group composed of 10 healthy mixed breed dogs (5 males and 5 females) aged between 2 and 11 years old.

### Preparation of animals for the SD-OCT

The SD-OCT and ERG examinations were performed at least 7 days apart. In all dogs, SD-OCT was performed between 9 a.m. and 1 p.m. Pupils were dilated using tropicamide eye drops (Tropicamidum WZF 1%, Polfa Warszawa S.A., Poland). The dogs were sedated with medetomidine 0.03 mg/kg (Cepetor 1 mg/mL, CP Pharma, Germany) administered intramuscularly. Local anesthesia of the corneal and conjunctival surface was achieved using 0.5% proxymetacaine hydrochloride (Alcaine 5 mg/mL, Alcon, Warsaw, Poland). A thumb forceps was used to grasp the bulbar conjunctiva and stabilize the eye. During the SD-OCT examination, the cornea was moistened every 30 s with saline.

### OCT scan and data analysis

The imaging was performed for both eyes of each animal using SD-OCT (wavelength: 840 nm; scan pattern: enhanced depth imaging, EDI; Topcon 3D OCT-2000, Topcon, Japan) with linear and cross-sectional radial scans. The device's software allowed precise location of the choroidal measurements in the scans obtained. The caliper function integrated with the OCT software was used to manually perform choroid

measurements. The measurements were performed as described previously (Zwolska et al., 2023) and applied to the respective layers of the choroid. The measurement sequence included, starting from the innermostlayer, the RPE-Bruch's membrane – choriocapillaris complex (RPE-BmCc) with tapetum lucidum in the tapetal fundus, the medium-sized vessel layer (MSVL), the large vessel layer with lamina suprachoroidea (LVLS), and whole choroidal thickness (WCT) – Fig. 1.

Choroidal thickness was defined as the vertical distance from the hyperreflective line of the RPE-Bruch's membrane complex to the hyperreflective line of the inner sclera surface. Measurements were taken in the dorsal and ventral regions at 5000-6000 μm from the optic disc. Temporal (T) and nasal (N) scans were taken at 4000–7000 μm from the optic disc. Temporal and nasal measurements were taken both in the tapetal (temporal: TempT, nasal: NasT) and nontapetal fundus (temporal: TempNT, nasal: NasNT). Measurements in the TempT and NasT regions were taken at 500-2000 μm dorsally from the border between the tapetal and nontapetal regions. Measurements in the temporal and nasal nontapetal regions were taken at 500-2000 μm ventrally from the border between the tapetal and nontapetal regions. In each region, three measurements were taken: at the center of the scan and at 1500 μm from the center to both left and right. The results of the three measurements were then averaged for each segment. To avoid variability, all the measurements were taken at the same time of day and verified by the same two authors.

### Statistical methods

Data normality was tested using Lillieforce's method and verified with the Shapiro-Wilk test. Significantly different comparisons were identified using the Mann-Whitney $U$ test. Analyses were performed using

Table 1. Results of vision examinations and neuro-ophthalmic tests in the RA dog group.

| Dog no. | Menace response R | Menace response L | Tracking reflex | Visual placing reflex | Obstacle course test Scotopic conditions | Photopic conditions | Pupillary light reflex R | L | Dazzle reflex R | L | Chromatic pupillary light reflex R RED | BLUE | L RED | BLUE |
|---|---|---|---|---|---|---|---|---|---|---|---|---|---|---|
| 1 | +/– | +/– | +/– | +/– | – | + | + | + | + | + | + | + | + | + |
| 2 | +/– | +/– | +/– | – | – | – | +/– | +/– | +/– | +/– | – | +/– | – | +/– |
| 3 | – | – | – | – | – | – | – | – | – | – | – | – | – | – |
| 4 | – | – | – | – | – | – | – | – | – | – | – | – | – | – |
| 5 | – | – | – | – | – | – | – | – | – | – | – | – | – | – |
| 6 | – | – | – | – | – | – | +/– | +/– | +/– | +/– | – | +/– | – | +/– |
| 7 | +/– | +/– | +/– | +/– | – | + | + | + | + | + | + | + | + | + |
| 8 | – | – | – | – | – | – | – | – | – | – | – | – | – | – |
| 9 | – | – | – | – | – | – | – | – | – | – | – | – | – | – |
| 10 | – | – | – | – | – | – | – | – | – | – | – | – | – | – |
| 11 | + | + | + | + | + | + | + | + | + | + | + | + | + | + |
| 12 | – | – | – | – | – | – | +/– | +/– | – | – | +/– | +/– | +/– | +/– |
| 13 | – | – | – | – | – | – | – | – | – | – | – | – | – | – |
| 14 | – | – | – | – | – | – | – | – | – | – | – | – | – | – |
| 15 | – | – | – | – | – | – | – | – | – | – | – | – | – | – |
| 16 | +/– | +/– | +/– | +/– | – | + | + | + | + | + | + | + | + | + |
| 17 | – | – | – | – | – | – | +/– | +/– | +/– | +/– | – | +/– | – | +/– |
| 18 | + | + | + | + | + | + | + | + | + | + | + | + | + | + |
| 19 | – | – | – | – | – | – | – | – | – | – | – | – | – | – |
| 20 | +/– | +/– | – | +/– | – | + | +/– | +/– | – | – | – | +/– | – | +/– |
| 21 | – | – | – | – | – | – | – | – | – | – | – | – | – | – |
| 22 | +/– | +/– | +/– | +/– | – | + | + | + | + | + | + | + | + | + |
| 23 | – | – | – | – | – | – | +/– | +/– | +/– | +/– | – | +/– | – | +/– |
| 24 | – | – | – | – | – | – | – | – | – | – | – | – | – | – |
| 25 | + | + | + | + | + | + | + | + | + | + | + | + | + | + |

Menace response, tracking reflex, visual placing reflex, dazzle reflex: (+) = present, (–) = absent, (+/–) = unclear (uncertain). Obstacle course test: (–) =dog had difficulty navigating the course, (+) = dog did not have difficulty navigating the course.
Pupillary light reflex, chromatic pupillary light reflex: (–) = mydriasis with absent pupillary light response (PLR),(+/–) =delayed PLR, (+) = normal PLR. Dazzle reflex: (+) = present, (–) = absent. Chromatic pupillary light reflex (cPLR): (+) = cPLR present, (–) = cPLR absent, (+/–) = delayed cPLR.

Statistica 10 software (TIBCO Software Inc.). Statistical significance was set at p≤0.05.

## Results

### Clinical examinations

Clinical examinations revealed no irregularities in any of the dogs included in the study. Complete blood counts and biochemistry results for all dogs were within reference ranges.

### Vision and neuro-ophthalmic tests

Only dogs that did not have any ophthalmological diseases or vision impairments were selected for the Control group. Vision and neuro-ophthalmic tests were normal in the Control group dogs. Incipient cortical cataracts were found bilaterally in one 8-year-old male and one 13-year-old male from the RA group. An 8-year-old male also had asteroid hyalosis. The results of vision examinations and neuro-ophthalmic tests in the RA group are presented in Table 1.

All the dogs in the RA group showed typical PRA symptoms which included tapetal hyperreflectivity,
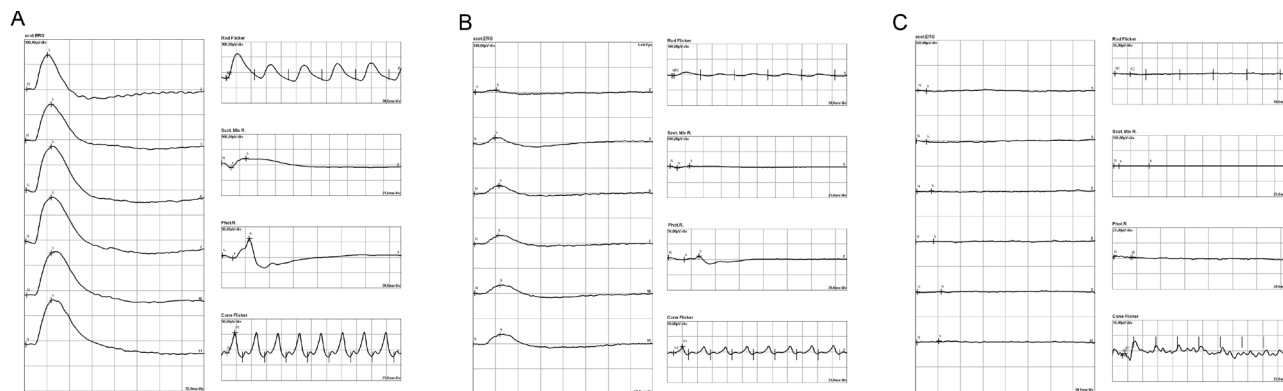
Fig. 2. Representative electroretinogram (ERG) waveforms recorded using the dog protocol for an animal from the control group (A), a dog in an early stage of RA (dog no. 11) (B), and a dog in an advanced stage of RA (dog no. 24) (C). The results in each column were obtained for the same dogs. The graphs present scotopic and photopic ERG.

vascular attenuation, abnormal pigmentation of the tapetal fundus, peripapillary halo, mottling, beading of retinal vessels, and ghost vessels. The changes were symmetrical and bilateral. In addition, the disease was confirmed by the ERG and SD-OCT examinations. Information obtained from the owners indicated that they had observed progressive vision impairment, initially in the scotopic condition.

### Electroretinographic examinations

The amplitude of the b-wave was significantly decreased at all light intensities in 11 RA cases (dog numbers 1,2,6,7,11,16,18,20,22,23,25). The a-wave amplitude was also significantly lower at all light intensities for the 11 RA-affected dogs. At the advanced stage of disease, in 14 dogs (dog numbers 3,4,5,8,9,10, 12,13,14,15,17,19,21,24), there were non-recordable extinguished (flatline) ERG responses for the scotopic and photopic ERGs.

Examples of scotopic and photopic responses: correct, decreased, and non-recordable ERG responses recorded for three dogs – one control group animal and two animals suffering from RA – respectively, in an early and advanced stage of the disease, are presented in Fig. 2.

### SD-OCT examinations

Measurement of choroidal layers in SD-OCT scans was possible in 22 of the 25 dogs suffering from RA. The results of these measurements were included in the statistical analysis. The scans of 3 dogs (no. 5, 9, and 14) were excluded as the advanced stage of the disease led to atrophy of the choroid and, consequently, it was impossible to distinguish the choroid or its respective layers (Fig. 3 – example scans).

Choroidal layer and whole choroidal thicknesses results for each respective region of the fundus are provided in Table 2. In all dogs affected by RA, there was a statistically significant reduction in thickness of MSVL compared to Control in all the regions measured. Statistically significant reduction in thickness of LVLS and WCT was found in all nontapetal areas in comparison to Control.

The advancement of the disease process in the nontapetal regions is visible in the scan (Fig. 4). The thickness of the LVLS and WCT layer in the nontapetal region was lower as compared to the scans obtained in the control group, as confirmed by the statistical analysis. The blurring of choroidal layers and choroidal atrophy was more severein the nontapetal regions.

## Discussion

The morphometric choroid analysis conducted in dogs suffering from RA revealed more advanced atrophy, i.e. more significant reduction in thickness of both LVLS and WCT layers, in all regions where the tapetum lucidum was not present, as compared to tapetal regions. As follows from our earlier research, retinal atrophy in dogs suffering from RA also begins in the ventral region, i.e. the region of the nontapetal fundus, from where it progresses above the optic nerve into the region of the tapetum lucidum (Balicki et al. 2018). This may suggest a direct connection between the advancement of the disease and changes developing in the large vessel layer with the lamina suprachoroidea, as well as reduction of overall choroidal thickness.

In the course of retinitis pigmentosa (RP), which is the human counterpart to canine PRA, choroid thickness changes in particular quadrants of the fundus. It was reported that in the human control group, the choroid was found to be thickest beneath the fovea and thinnest in the nasal quadrants. Whereas in the case of patients suffering from RP, the choroid was the thickest in the temporal quadrants, and the thinnest in the nasal quadrants (Adhi et al. 2013). In our study, it was
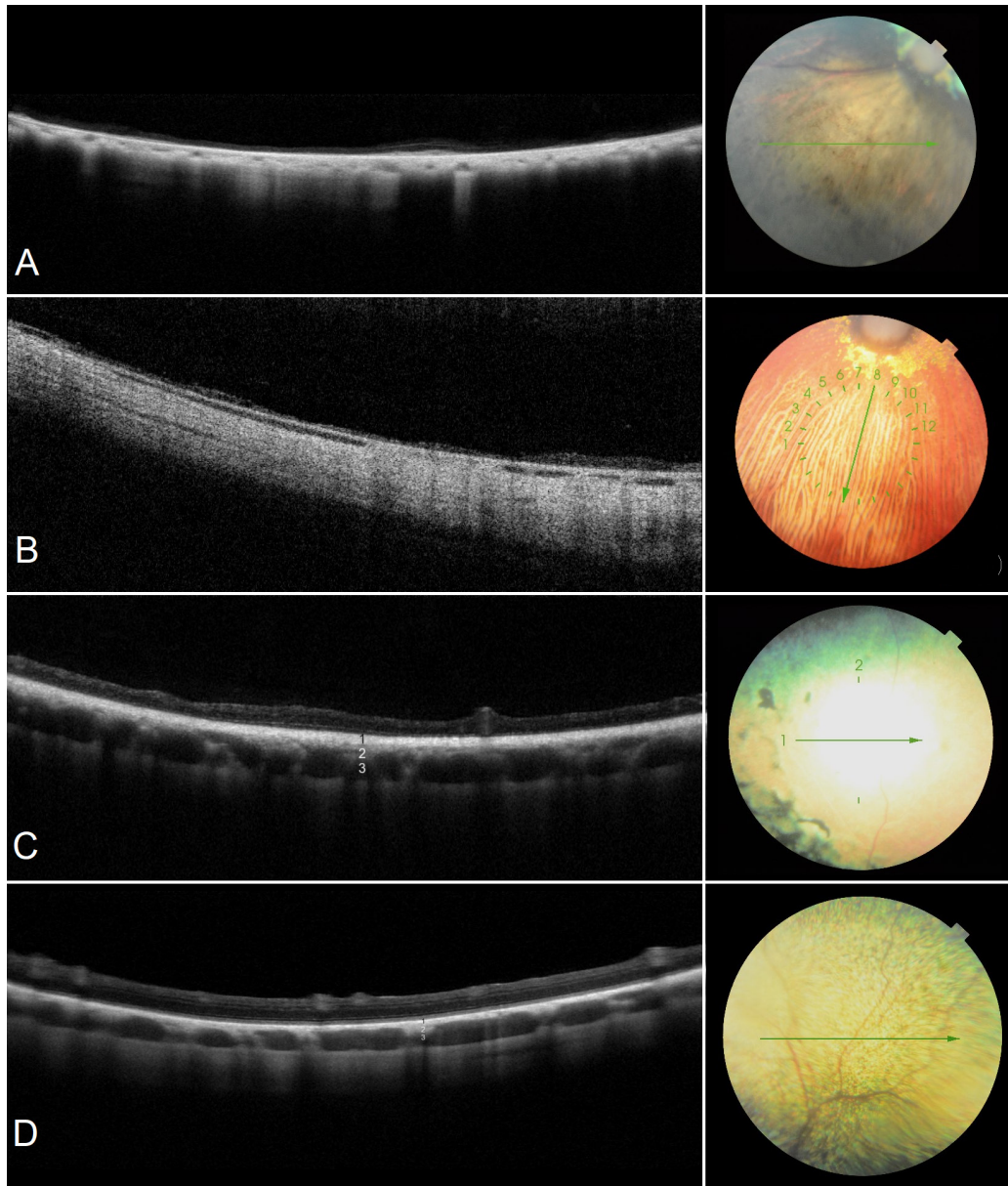
Fig. 3. Images of the retina and the choroid in various stages of the disease. Measurement of the choroid and its respective layers was impossible in the most advanced stage – A (dog no. 9), B (dog no. 14). In scans C – dog no. 2 and D – dog no. 25 the respective choroidal layers are visible: 1 – RPE-BmCc, 2 – MSVL, 3- LVLS.

demonstrated that in the case of dogs suffering from RA, the WCT was, similarly to the control group, thickest in the TempT region followed by the D region, and thinnest in the V region. At the same time, a statistically significant reduction in thickness of the WCT was observed in all nontapetal regions of the fundus. In the context of RP, difficulties were reported in terms of distinguishing the respective layers of the choroid (Adhi et al. 2013). In the control group, the imaging clearly showed the choriocapillary vessels, medium-sized and large blood vessels. Meanwhile, in patients suffering from RP, it proved difficult to distinguish the choriocapillaris from the medium-sized vessel layer in the scans. Nonetheless, the joint thickness of the two layers was used to

estimate mean thickness changes. The thickness analyses evidenced reduction in thickness of the large vessel layer, while the joint thickness of the choriocapillaris and medium-sized vessel layers remained unaffected (Adhi et al. 2013). In our study conducted on dogs, the particular choroidal layers were indistinguishable in the most advanced cases of RA due to the simultaneous atrophy of the retina. Dogs in the advanced stage of retinal and choroidal atrophy had to be excluded from the measurements due to the impossibility of measuring the respective layers. In the remaining dogs, however, the results revealed reduction in thickness of the MSVL layer in all the analyzed regions. Reduction in thickness of the LVLS and WCT layers was registered only in the
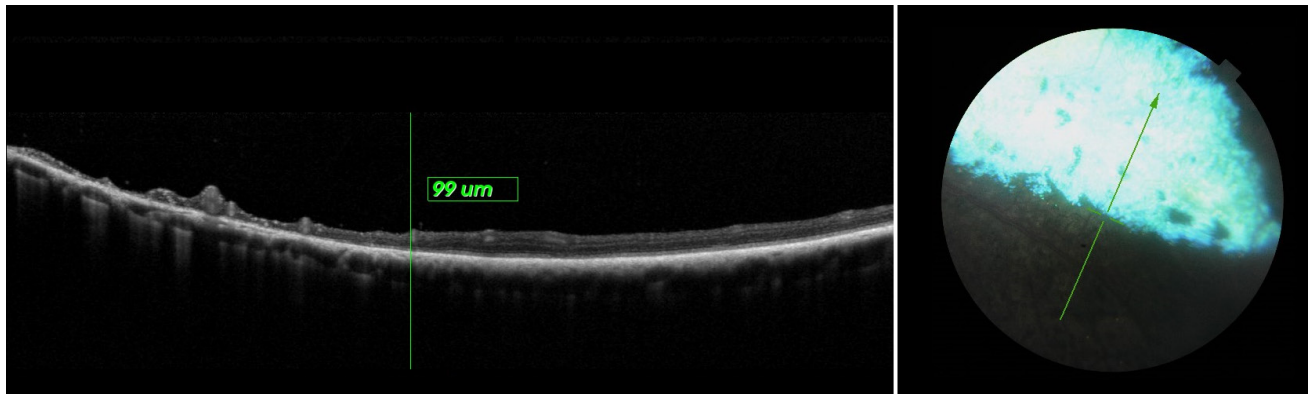
Fig. 4. Scan presenting the different stages of retinal and choroidal atrophy advancement relative to the presence of the tapetum lucidum (dog no. 20). Significant advancement of retinal and choroidal atrophy in the nontapetal region. The green arrow in the fundus photograph indicates the location of the scan. The short green line on the border of the tapetal and nontapetal region, perpendicular to the green arrow in the fundus photograph corresponds to the green vertical line visible in the scan.

Table 2. Choroidal layers and whole choroidal thicknesses (median ($\mu$m) [minimum (Min) - maximum (Max)]) in certain fundus regions in the Control and RA dog groups.

| | Fundus region | | | |
|---|---|---|---|---|
| Layer | D | | V | |
| | Control | RA | Control | RA |
| RPE-BmCc | 29.17 [19.00-39.33] | 22.33 [10-37.50]* | 7.67 [6.33-9.33] | 8.18 [7.00-9.17]* |
| MSVL | 32.25 [22.00-44.60] | 24.75 [8.83-38.0]* | 24.20 [15.67-36.17] | 15.00 [12.50-25.00]* |
| LVLS | 120.80 [89.50-170.67] | 118.17 [58.83-174.83] | 71.00 [57.00-113.50] | 51.00 [19.00-88.67]* |
| WCT | 190.50 [134.83-222.83] | 163.00 [79.67-237.17] | 104.00 [80.67-153.00] | 75.83 [26.33-116.33]* |
| Layer | TempT | | TempNT | |
| | Control | RA | Control | RA |
| RPE-BmCc | 10.00 [7.33-15.67] | 10.00 [8.33-15.17] | 7.67 [7.00-9.40] | 8.33 [7.00-12.00] |
| MSVL | 49.00 [36.50-69.33] | 34.20 [11.33-51.67]* | 30.00 [15.00-39.50] | 15.92 [9.33- 24.42]* |
| LVLS | 138.67 [80.50-171.33] | 125.00 [62.00-171.33] | 87.00 [63.00-110.33] | 62.00 [38.00-113.00]* |
| WCT | 202.50 [125.50-223.67] | 164 [83.33-219.00] | 119.50± [85.00-147.67] | 86.00 [55.00-146.00]* |
| Layer | NasT | | NasNT | |
| | Control | RA | Control | RA |
| RPE-BmCc | 10.33 [7.50-12.00] | 10.50 [8.50-11.50] | 7.67 [7.00-9.75] | 8.17 [7.00- 0.67] |
| MSVL | 35.00 [27.33-40.50] | 22.67[19.00-30.33]* | 30.00 [16.67-43.00] | 18.52 [12.67-23.67]* |
| LVLS | 92.00 [76.00-110.00] | 94.67 [74.67-113.00] | 89.67 [71.00-110.00] | 70.67 [44.50-106.00]* |
| WCT | 139.50 [123.60-151.33] | 130.33 [104.17-148.50] | 123.00 [95.33-162.00] | 97.42 [54.50-140.00]* |

D – dorsal, V – ventral, TempT – temporal tapetal, TempNT – temporal nontapetal, NasT – nasal tapetal, NasNT – nasal nontapetal.

nontapetal regions where more advanced retinal atrophy was also observed, as compared to the tapetal regions.

The present study does not explain whether the reduction of thickness of choroidal layers was primary or secondary to retinal atrophy. The research indicated that in the case of advanced retinal atrophy, both structures were completely atrophied (Fig. 3). Both the retina and the choroid are tissues that complement each other. The choroid synthesizes a number of growth factors involved in angiogenesis, such as vascular endothelial growth factor (VEGF), and signal molecules. It was found that trophic factors from the choroid were necessary for the development and survival of the ciliary ganglion neurons (Nickla and Wallman 2010). Demonstrating which structure atrophied first and led to the atrophy of the other structure in case of RA needs further detailed research.

Studies conducted on mice evidenced the particular importance of the VEGF factor produced in the retinal

pigmental epithelium - capable of diffusion across Bruch's membrane – in maintaining the choriocapillaris. In animals that produce only VEGF isoforms with low ability to permeate Bruch's membrane, and not the isoforms capable of diffusion towards the choriocapillaris, correct initial development of the choroid was observed. However, over time – starting from the 7th month of a mouse's life – atrophy of the choriocapillaris was reported, as well as disorders related to Bruch's membrane and the pigmental epithelium, degeneration of the choroid, and an increased number of non-vascularized areas in the region. This led to eventual photoreceptor apoptosis, as evidenced in electroretinographic imaging. The limitation of the cited studies stemmed from the fact that they only analyzed whole choroid thickness without considering its respective layers (Saint-Geniez et al. 2009, Liu et al. 2016). An interesting observation in the present study was that a significant decrease in the WCT thickness was registered only in the nontapetal regions where tapetum lucidum was not present. In a study conducted by Lesiuk and Braekevelt (1983), differences in the thickness of Bruch's membrane were evidenced between respective regions of the choroid. Over the areas with tapetum lucidum, Bruch's membrane was thinner compared to its thickness over the areas where it was not present. It could be posited that the higher rate of morphometric and morphological choroidal lesions in the nontapetal regions may be related to the greater thickness of Bruch's membrane in the area, and consequently its reduced permeability for growth factors produced by the retinal pigment epithelium (RPE). This may be one of the factors contributing to the pathomechanism of PRA, although further research is required to corroborate this.

Branches of fenestrated capillaries pass through the entire tapetum lucidum. They serve as the link between the choriocapillaris and the layer of medium-sized blood vessels (Sattler's layer). The choriocapillaris is a vast anastomosing network of blood vessels located in the vicinity of the retinal pigmental epithelium. Near the RPE, the layout of these vessels differs between the choroidal regions containing the tapetum lucidum (tapetal and peritapetal areas) and the regions where it is absent (peripheral nontapetal areas). In the case of locations where the reflective membrane is present, the choriocapillaris indents the retinal epithelium, which does not occur in areas where the tapetum lucidum is not present (Lesiuk and Braekevelt. 1983). This is yet another anatomical element of the canine eye that may potentially account for the greater severity of the symptoms of the disease in areas not containing the tapetum lucidum. The previously demonstrated lack of direct contact between the choriocapillaris and the external layers of the choroid in the nontapetal region may be related to the greater progression of outer choroidal atrophy in those areas.

The limitations of the study reported here were typical of retrospective studies. The study does not allow which structure, retina or choroid, atrophied first, to be determined, which requires further detailed research. Despite these limitations, this study aimed to analyze the morphometrics of the choroid without considering the retina. Subsequent work may include research on the relationship between retinal atrophy and the choroid, which would include a larger research group allowing for the identification of quantitatively homogenous subgroups with a similar degree of retinal atrophy.

## Conclusion

This studyis the first to consider morphological and morphometric choroidal changes observed in dogs suffering from RA. RA in mixed breed dogs was accompanied by reduction of the thickness of the large vessel layer and overall choroidal thickness in the nontapetal fundus as well as the medium vessel layer in all fundus regions. Our research showed a change in choroidal layer thicknesses in dogs diagnosed with RA, which can affect the outer retinal blood supply. SD-OCT analyses of choroidal thickness profiles may shed a new light on the pathomechanism of RA and form the basis for further research to be continued in purebred dogs.

## Acknowledgements

## References

Adhi M, Regatieri CV, Branchini LA, Zhang JY, Alwassia AA, Duker JS **(2013)** Analysis of the Morphology and Vascular Layers of the Choroid in Retinitis Pigmentosa Using Spectral-Domain OCT. Ophthalmic Surg Lasers Imaging Retina 44: 252-259.

André C, Chaudieu G, Thomas A, Jongh O, Jegou JP, Chahory S, Clerc B, Pilorge P, Brenac O **(2008)** Hereditary retinopathies in the dog: Genetic fundamentals and genetic tests. Pratique Médicale et Chirurgicale de l'Animal de Compagnie 43: 75-84.

Balicki I, Szadkowski M, Balicka A, Lew M, Trbolova A **(2018)** Assessment of generalized progressive retinal atrophy (GPRA) in mixed breed dogs using spectral domain optical coherence tomography (SD-OCT) and electroretinography. Abstracts: Annual Scientific Meeting of the European College of Veterinary Ophthalmologists, Florence, Italy May 10-13, 2018. Veterinary Ophthalmology Vol. 21 Issue 5.

Barnett K C, Curtis R, Millichamp N J **(1983)**: The differential diagnosis of retinal degeneration in the dog and cat. J Small Anim Pract 24: 663-673.

Bruè C, Mariotti C, De Franco E, Fisher Y, Guidotti JM, Giovannini A **(2013)** Solar Retinopathy: A Multimodal Analysis. Case Rep Ophthalmol Med 2013: 906920.

Brusini P **(2018)** OCT Glaucoma Staging System: a new method for retinal nerve fiber layer damage classification using spectral-domain OCT. Eye (Lond) 32: 113-119.

Downs LM, Hitti R, Pregnolato S, Mellersh CS **(2014)** Genetic screening for PRA -associated mutations in multiple dog breeds shows that PRA is heterogeneous within and between breeds. Vet Ophthalmol 17: 126-130.

Ekesten B, Komáromy AM, Ofri R, Petersen-Jones SM, Narfström K **(2013)** Guidelines for clinical electroretinography in the dog: 2012 update. Doc Ophthalmol 127: 79-87.

Finzi A, Cellini M, Strobbe E, Campos EC **(2014)** ET-1 plasma levels, choroidal thickness and multifocal electroretinogram in retinitis pigmentosa. Life Sci 118: 386-390.

Gabriele ML, Wollstein G, Ishikawa H, Kagemann L, Xu J, Folio LS, Schuman JS **(2011)** Optical Coherence Tomography: History, Current Status, and Laboratory Work. Invest Ophthalmol Vis Sci 52: 2425-2436.

Korte GE, Reppucci V, Henkind P **(1984)** RPE Destruction Causes Choriocapillary Atrophy. Invest Ophthalmol Vis Sci. 25: 1135-1145.

Lesiuk TP, Braekevelt CR **(1983)** Fine structure of the canine tapetum lucidum. J Anat. 136: 157-164.

Liu G, Liu X, Li H, Du Q, Wang F **(2016)** Optical Coherence Tomographic Analysis of Retina in Retinitis Pigmentosa Patients. Ophthalmic Res 56: 111-122.

Maggs D, Miller P, Ofri R **(2017)**. In: Slatter's Fundamentals of Veterinary Ophthalmology (6th ed.). Elsevier Health Sciences, St. Louis, pp 362-372.

McLellan GJ, Rasmussen CA **(2012)** Optical coherence tomography for the evaluation of retinal and optic nerve morphology in animal subjects: practical considerations. Vet Ophthalmol 15 (Suppl 2): 13-28.

Milam AH, Li ZY, Fariss RN **(1998)** Histopathology of the Human Retina in Retinitis Pigmentosa. Prog Retin Eye Res 17: 175-205.

Murthy RK, Haji S, Sambhav K, Grover S, Chalam KV **(2016)** Clinical applications of spectral domain optical coherence tomography in retinal diseases. Biomed J 39: 107-120.

Nickla DL, Wallman J **(2010)** The multifunctional choroid. Prog Retin Eye Res 29: 144-168.

Oh JK, Nuzbrokh Y, Lima de Carvalho JR Jr, Ryu J, Tsang SH **(2020)** Optical coherence tomography in the evaluation of retinitis pigmentosa. Ophthalmic Genet 41: 413-419.

Poornachandra B, Khurana AK, Sridharan P, Chatterjee P, Jayadev C, Yadav NK, Shetty R **(2019)** Quantifying micro-structural changes in retinitis pigmentosa using spectral domain - optical coherence tomography. Eye Vis (Lond) 6: 13.

Rosolen SG, Rivière ML, Lavillegrand S, Gautier B, Picaud S, LeGargasson JF **(2012)** Use of a combined slit-lamp SD-OCT to obtain anterior and posterior segment images in selected animal species. Vet Ophthalmol 15 (Suppl 2): 105-115.

Saint-Geniez M, Kurihara T, Sekiyama E, Maldonado AE, D'Amore PA **(2009)** An essential role for RPE-derived soluble VEGF in the maintenance of the choriocapillaris. Proc Natl Acad Sci USA 106: 18751-18756.

Shintani K, Shechtman DL, Gurwood AS **(2009)** Review and update: Current treatment trends for patients with retinitis pigmentosa. Optometry 80: 384-401.

Singh SR, Vupparaboina KK, Goud A, Dansingani KK, Chhablani J **(2019)** Choroidal imaging biomarkers. Surv Ophthalmol 64: 312-333.

Xu J, Wang YX, Jiang R, Wei WB, Xu L, Jonas JB **(2017)** Peripapillary choroidal vascular layers: the Beijing Eye Study. Acta Ophthalmol 95: 619-628.

Zwolska J, Balicki I, Balicka A **(2023)** Morphological and Morphometric Analysis of Canine Choroidal Layers Using Spectral Domain Optical Coherence Tomography. Int J Environ Res Public Health 20: 3121.

Zwolska J, Szadkowski M, Balicka A, Balicki I **(2021)** Morpho-metrical analysis of the canine choroid in relation to age and sex using spectral domain optical coherence tomography. Acta Vet Hung 69: 266-273.